CANADIAN APPLIED
MATHEMATICS QUARTERLY
Volume 10, Number 3, Fall 2002

ELECTROMAGNETIC WELLBORE HEATING

Based on work from the Fourth Annual Industrial Problem Solving Workshop, June 2000.

C. SEAN BOHUN, BRUCE MCGEE AND DAVID ROSS

ABSTRACT. A model is proposed for the flow of fluids in a horizontal well that is electrically heated from an external source. By analysing the physical processes involved, a second order nonlinear ODE is derived for the volume flux of the well as a function of distance along the wellbore. Comparing the extracted average radial temperature and pressure profiles with a commercial CFD solver illustrates that this simplified model captures much of the structure involved in the solution to the full PDE solution.

1 Introduction. In this paper we derive a simple model that describes the recovery of petroleum fluids from an oil reservoir by the method of electromagnetic heating. By its very nature this problem must deal with both the equations that describe the fluid flow as well as the heat flow. In fact, one approach to this problem is to write out the full system of coupled partial differential equations that relate the temperature and the velocity flux and then to solve them numerically with a computational fluid dynamics (CFD) program. This method has been used in the past [**5**] and the results from a commercial CFD solver will be used to test the accuracy of our simplified model in the absence of experimental data.

In general, the oil in the wellbore is very viscous with the consequence that the fluid moves slowly. As a result, the amount of oil collected in a given time is quite small. To increase the production rate of the well,

Accepted for publication on December 16, 2001.
AMS subject classification: 80A20, 35Q35, 76R99.
Keywords: electrical heating, incompressible viscous flow, heat flow, horizontal well.

the oil's velocity needs to be increased, and one method of accomplishing this is by heating the fluid using an electromagnetic induction tool (EMIT). The simple principle behind the EMIT is that it heats the fluid, thereby decreasing its viscosity and increasing its velocity. This method of increasing the production rate of a given wellbore is currently being utilized with the generalization that for wells of several hundred meters in length, several EMIT regions are placed in the wellbore at intervals of about one hundred meters. So that they are all supplied sufficient power, these EMIT regions are connected by a cable surrounded by a steel housing.

The purpose of this paper is to carefully analyze each of the physical processes in this system, and by making some basic assumptions to derive a simple set of equations that can be solved rapidly while still capturing the main features of the system modelled with the CFD code. In this process we find that under our assumptions, the flux of oil from the wellbore can be modelled with a single nonlinear second order boundary value problem.

For comparison of the two models, the production rate at the pump was computed for each model in the unheated case. The difference between them was found to be less than 5%. This is quite remarkable considering the relative complexity of the two models. When the wellbore is heated the deviation between the CFD package and our solution increases, but it does so in a manner consistent with the formation of a thermal boundary layer at the wellbore casing. Since the commercial code is time dependent and does not model the wellbore as an idealized pipe, the comparison in this heated case required many hours of computation. As such only one iteration of the CFD solution was pursued.

One of the advantages of the simplified model is that it allows one to search wide ranges of parameter space. With a large commercial package this procedure can be prohibitively expensive. We consider two problems along these lines. First, we determine the production rate at the pump as a function of position in the wellbore and the amount of power applied. Second, the rule of thumb of placing the EMIT regions at 100 m intervals in a long well is analyzed.

This paper is organized in the following way. Section 2 describes the overall geometry of the problem and establishes the coordinates used to describe the model. At this point the problem is broken into three subproblems: (i) the radial flow of fluid in the reservoir, (ii) the horizontal flow of fluid in the wellbore and (iii) the generation of temperature from the heat sources in any EMIT regions and how this couples to parts (i) and (ii). Parts (i) and (ii) result in a second order ODE for the radially

average oil flux determined at a fixed viscosity. From part (iii) it is found that the temperature of the fluid is inversely proportional to the velocity. Consequently, fluid that moves slowly past an EMIT region will absorb more heat than the same amount of fluid that moves quickly past an EMIT. As a result, slowing the fluid velocity increases the temperature and therefore decreases the viscosity. This viscosity is used in parts (i) and (ii) to close the system of equations.

Part (i) is described in Section 3, where a relationship between the axial changes in the fluid flux and the pressure in the wellbore is derived. The details of part (ii) can be found in Section 4 where a relationship for the velocity and the pressure from the Navier-Stokes equations is obtained by averaging over the radius of the wellbore. Under the assumptions made, the pressure is found to be related to the radius of the wellbore by a form of Poiseuille's law. Section 5 illustrates the analytical solution of the resulting model in the simple situation when no heat is applied to the oil.

Section 6 details the derivation of part (iii), the temperature equations. This derivation is complicated by the fact that there are four radial regions of the radial problem to consider: EMIT, casing, reservoir and wellbore, with the first three forming the boundary conditions for the heat equation in the wellbore region. Furthermore, there are three axial regions: EMIT region, cable region, and a region where there is neither EMIT nor cable. Section 7 summarizes resulting nonlinear ODE obtained by pulling the results of Sections 3, 4 and 6 together.

In Section 8, we discuss the numerical results of the simplified model and how they compare to the results predicted by the CFD code. On comparison, we find considerable qualitative agreement between the two models. These aspects are further discussed in the final section of the paper.

2 Geometry. Figure 1 depicts the overall geometry of the problem. A horizontal cylindrical well extends from $z = 0$ to $z = L$. Fluid flows radially into the well from the surrounding media and is drawn out with a pump which is located at $z = L$ where a fixed producing pressure of P_P is maintained.

At $z = 0$, where the end cap is situated, the motion of the flow is radially inward through the reservoir and the casing that lines the complete length of the wellbore (no horizontal flow at this point). As z increases, the action of the pump comes into effect and imparts a horizontal component to the fluid flow.

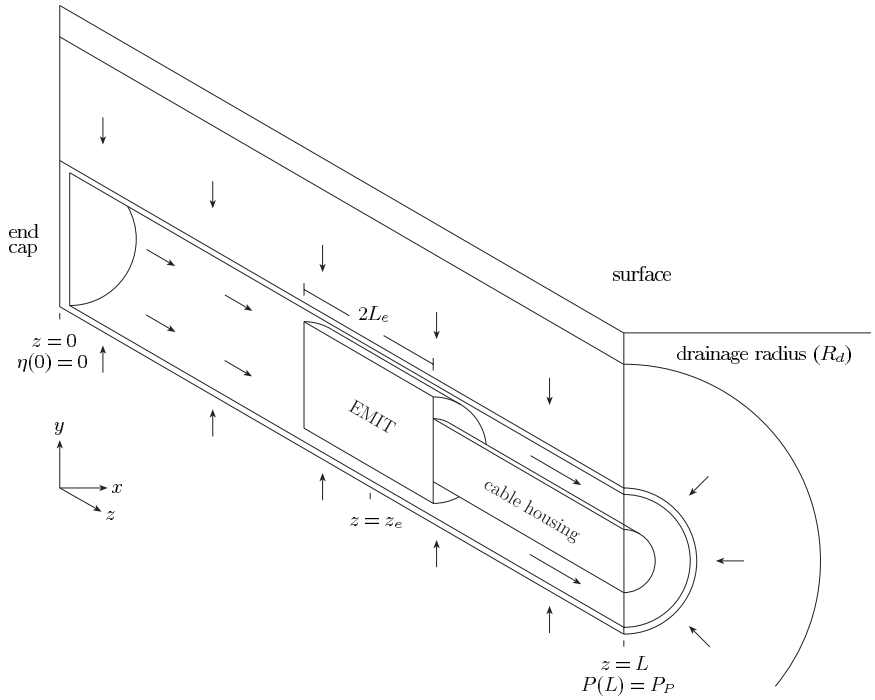

FIGURE 1: Cross section of the overall geometry for the horizontal wellbore problem. The rate and direction of the oil flow is indicated with the arrows. At $z = 0$ there is an end cap and the horizontal flow is zero while at $z = L$ there is a pump that maintains the producing pressure P_P.

This figure shows only one EMIT region located at $z = z_e$ of length $2L_e$ but the analysis can be easily generalized to the case of N EMIT regions. It is in these EMIT regions that the oil is heated. The casing in these regions acts as a single turn secondary winding of a transformer thereby heating the surrounding fluids. Power is supplied to the EMITs through a cable housing resulting in three different regions. Starting at the end cap the wellbore is open with no impediment to the horizontal flow. This extends to the first EMIT. If there are other EMIT regions then they must also be joined with cable housing and eventually, after the last EMIT region, we have a cable housing region that extends to the pump.

There are a number of physical constants associated with the fluid and heat flow within the wellbore. Since these are required to generate

numerical solutions and to justify some of the assumptions, they have been collected in Table 1.

3 Axial velocity: Darcy's Law. Once the horizontal well is drilled, fluid seeps from the surrounding region into the wellbore. Having reached the wellbore, the fluid is drawn out with a pump that maintains a fixed pressure at one end of the well. The rate at which the fluid seeps into the wellbore is a function of the pressure differential and the viscosity of the fluid. Indeed, the flow rate (volume/time) of the fluid into a segment of the wellbore of length Δz is given by the expression [**3**]

$$q(z) = \frac{2\pi k[P_R - P(z)]}{\mu_o \ln(R_d/R_c)}\Delta z \tag{1}$$

where k is the permeability of the reservoir, P_R is the reservoir pressure and $P(z)$ is the pressure inside the wellbore at the axial position z. As well, μ_o is the viscosity at the ambient temperature T_a and R_d/R_c is the ratio of the drainage radius to the outer radius of the casing.

Since we are assuming that we are at a steady state, we make the assumption that the radially flowing fluid remains unheated until it reaches the outer radius of the casing at which point it instantly becomes heated to the average temperature of the fluid at that particular z position. Consequently the viscosity in expression (1) will remain as μ_o even when the temperature of the wellbore is increased.

Using equation (1) one can find an expression for the average axial velocity of the fluid, $\bar{v}(z)$. Let R_z denote the inner radius of the wellbore which depends on the axial region under consideration. For one EMIT region with R_e the radius of the EMIT and letting R_h denote the outer radius of the electrical housing

$$R_z = \begin{cases} 0, & 0 \le z < z_e - L_e \\ R_e, & z_e - L_e \le z \le z_e + L_e \\ R_h, & z_e + L_e < z \le L \end{cases} \tag{2}$$

so that $\eta(z) = \pi(R_w^2 - R_z^2)\bar{v}(z)$ is the flux in the wellbore. The advantage of using $\eta(z)$ rather than $\bar{v}(z)$ is that $\eta(z)$ is a continuous function whereas the velocity $\bar{v}(z)$ is not.

[1] 1 darcy $= 9.86923 \times 10^{-13}$ m^2.
[2] 1 centipoise $= 1 \times 10^{-3}$ kg m^{-1}s^{-1}.
[3] 1 pascal $= 1$ kg m^{-1}s^{-2}.

Data	Symbol	Value
Wellbore Properties		
Outer Casing Radius	R_c	69.85 mm
Inner Casing Radius	R_w	63.50 mm
EMIT Radius	R_e	50.80 mm
Housing Radius	R_h	30.1625 mm
Centre of the EMIT	z_e	500 m
EMIT Length	$2L_e$	10 m
Wellbore Length	L	1,000 m
Reservoir Properties		
Permeability[1]	k	10,000 mD
Ambient Viscosity[2]	μ_o	15,000 cP
Drainage Radius	R_d	100 m
Reservoir Pressure[3]	P_R	5,000 kPa
Producing Pressure	P_P	500 kPa
Thermal Properties		
Fluid Heat Capacity	ρC_f	2.8×10^6 J m^{-3}K^{-1}
Casing Power	Q_c	795.8 kW m^{-3}
EMIT Power	Q_e	79.58 kW m^{-3}
Ambient Temperature	T_a	30°C

TABLE 1: Input data for the example calculations.

Figure 2 shows an infinitesimal annular section of the wellbore of length Δz. At $z = z_*$ the axial flux is $\eta(z_*)$ while the radial flux is given by expression (1). By the conservation of mass, these two components combine to give the axial flux at $z = z_* + \Delta z$. In other words,

$$\eta(z_*) + \frac{2\pi k[P_R - P(z_*)]}{\mu_o \ln(R_d/R_c)}\Delta z = \eta(z_* + \Delta z).$$

Rearranging terms and letting $\Delta z \to 0$ gives the expression

$$\frac{d\eta}{dz} = \frac{2\pi k[P_R - P(z)]}{\mu_o \ln(R_d/R_c)}; \quad \eta(0) = 0. \tag{3}$$

The boundary condition $\eta(0) = 0$ just expresses our approximation that the axial fluid velocity is zero at the end cap of the wellbore. Since $P(z) < P_R$ throughout the wellbore, $d\eta/dz > 0$, which is consistent with having the fluid flux increase as it approaches the pump located at $z = L$.

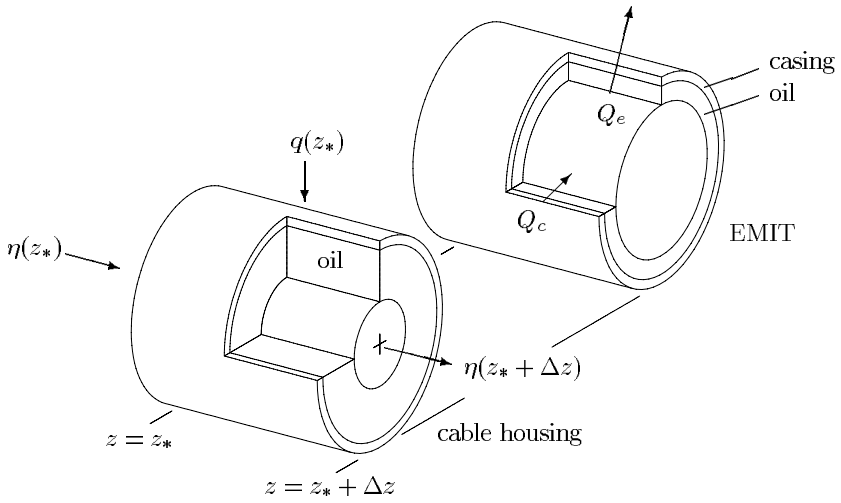

FIGURE 2: An infinitesimal section of the wellbore for the EMIT or cable housing regions.

4 Axial pressure: Navier-Stokes. A relationship between wellbore pressure and flow velocity is obtained from the Navier-Stokes equations for an incompressible viscous fluid,

$$\rho\frac{\partial\vec{v}}{\partial t}+\rho(\vec{v}\cdot\nabla)\vec{v}=-\nabla P+\mu\Delta\vec{v}. \tag{4}$$

Again refer to Figure 2, where we consider an arbitrary yet constant cross-section. Assume a steady fluid flow inside the wellbore that propagates in the $\hat{\mathbf{k}}$ direction. Assuming that the flow is radially symmetric, we have $\vec{v}=v(r)\hat{\mathbf{k}}$, and the continuity equation is automatically satisfied. Resolving (4) into the r, θ and z directions gives $\partial P/\partial r=0=\partial P/\partial\theta$ and

$$\mu\frac{1}{r}\frac{\partial}{\partial r}\Big(r\frac{\partial v}{\partial r}\Big)=\frac{\partial P}{\partial z}. \tag{5}$$

The first two conditions on the pressure imply that $P=P(z)$. As a consequence, the RHS of (5) is a function of z alone while the LHS is a function of r alone. The only way that this can be so is if the pressure is constant over the cross-section of the wellbore. This implies that for our annular domain $R_z\le r<R_w$ and $z_*<z<z_*+\Delta z$ we must solve

$$\mu\frac{1}{r}\frac{\partial}{\partial r}\Big(r\frac{\partial v}{\partial r}\Big)=\frac{\Delta P}{\Delta z};\quad v(R_z)=0,\ v(R_w)=0$$

where $\Delta P = P(z_* + \Delta z) - P(z_*) < 0$. At the inner radius R_z we have imposed a no-slip condition which is replaced with $v(0) < \infty$ when $R_z = 0$. Because the casing is perforated to allow fluids to easily pass,[4] it is not a solid boundary, and as such the possibility of a small axial velocity v_ϵ at the inner casing wall R_w, is conceded. However, we impose a no-slip condition at the inner casing since the effect of this small velocity is to simply add a constant flux to η. The general solution for the velocity distribution as a function of radius is found to be

$$v(r) = \frac{1}{4\mu}\frac{\Delta P}{\Delta z}\Big[r^2 - R_w^2 + \frac{R_w^2 - R_z^2}{\ln(R_z/R_w)}\ln\Big(\frac{r}{R_w}\Big)\Big].$$

For regions in which there is no EMIT tool or tubing ($R_z = 0$), this reduces to the familiar parabolic flow profile

$$v(r) = \frac{1}{4\mu}\frac{\Delta P}{\Delta z}(r^2 - R_w^2).$$

In order to find the average flux of oil at any fixed value of z, one needs to compute the average of this radial velocity. Computing this average results in

$$\overline{v} = \frac{2}{(R_w^2 - R_z^2)}\int_{R_z}^{R_w} v(r)r\,dr = -\frac{R_w^2}{8\mu}\frac{\Delta P}{\Delta z}\Big(\frac{1-\lambda^2}{\ln\lambda} + \frac{1-\lambda^4}{1-\lambda^2}\Big)$$

where $\lambda = R_z/R_w$ and $0 \le \lambda < 1$. If we now let $\Delta z \to 0$, rearrange terms and use the definition of η, this becomes

$$\frac{dP}{dz} = -\frac{8\mu}{\pi R_w^4}\Big[\frac{\ln\lambda}{(1-\lambda^2)^2 + (1-\lambda^4)\ln\lambda}\Big]\eta(z); \quad P(L) = P_P \tag{6}$$

where P_P is the pressure maintained by the pump at $z = L$. If one allows $\lambda \to 0^+$ ($R_z \to 0^+$) then equation (6) reduces to the popular *Hagen-Poiseuille* [**1**] equation,

$$\frac{dP}{dz} = -\frac{8\mu}{\pi R_w^4}\eta(z).$$

Differentiating expression (3) and using (6) we obtain a second order equation for the flux

$$\begin{gathered}\frac{d^2\eta}{dz^2} - \gamma^2(z)\frac{\mu}{\mu_o}\eta = 0;\\ \gamma^2(z) = \frac{16k}{R_w^4\ln(R_d/R_c)}\Big[\frac{\ln\lambda}{(1-\lambda^2)^2 + (1-\lambda^4)\ln\lambda}\Big]\end{gathered} \tag{7}$$

[4]The casing actually has holes drilled into it for the transport of oil.

with boundary conditions

$$\eta(0) = 0, \quad \frac{d\eta}{dz}\Big|_L = \frac{2\pi k(P_R - P_P)}{\mu_o \ln(R_d/R_c)}. \tag{8}$$

Notice that γ^2 is both positive and piecewise constant.

5 An illustrative example. Before we consider what happens as the wellbore is heated, it is instructive to consider the unheated case with no EMIT regions. Since no heat is applied, the viscosity of the fluids in the wellbore will be the same as those in the surrounding medium. In addition, $R_z = 0$ throughout the wellbore so that the equation for $\eta(z)$ reduces to

$$\frac{d^2\eta}{dz^2} - \gamma^2\eta = 0; \quad \eta(0) = 0, \quad \frac{d\eta}{dz}\Big|_L = \frac{2\pi k(P_R - P_P)}{\mu_o \ln(R_d/R_c)}.$$

The explicit form of the solution is easily verified to be

$$\eta(z) = \frac{\pi R_w^4}{8\mu_o}\frac{P_R - P_P}{L_{\text{crit}}}\frac{\sinh\gamma z}{\cosh\gamma L}; \quad L_{\text{crit}}^2 = \frac{R_w^4}{16k}\ln\Big(\frac{R_d}{R_c}\Big) = \frac{1}{\gamma^2}.$$

From expression (3) the corresponding pressure is

$$P(z) = P_R - (P_R - P_P)\frac{\cosh\gamma z}{\cosh\gamma L}.$$

The total production rate at the pump is given by the revealing expression

$$\eta(L) = \frac{\pi R_w^4}{8\mu_o}\frac{P_R - P_P}{L_{\text{crit}}}\tanh\gamma L \sim \begin{cases} \dfrac{\pi R_w^4}{8\mu_o}\dfrac{P_R - P_P}{L_{\text{crit}}}\dfrac{L}{L_{\text{crit}}}, & L \ll L_{\text{crit}} \\ \dfrac{\pi R_w^4}{8\mu_o}\dfrac{P_R - P_P}{L_{\text{crit}}}, & L \gg L_{\text{crit}} \end{cases}$$

which is depicted in Figure 3 for the data given in Table 1 where $L_{\text{crit}} = 865$ m and the maximum production rate is 191.32 m^3/day. What is immediately apparent is that, without heating, drilling a horizontal well beyond the critical length will not yield any significant increase in production.

We have now reached the point where we can consider what happens as the wellbore is heated.

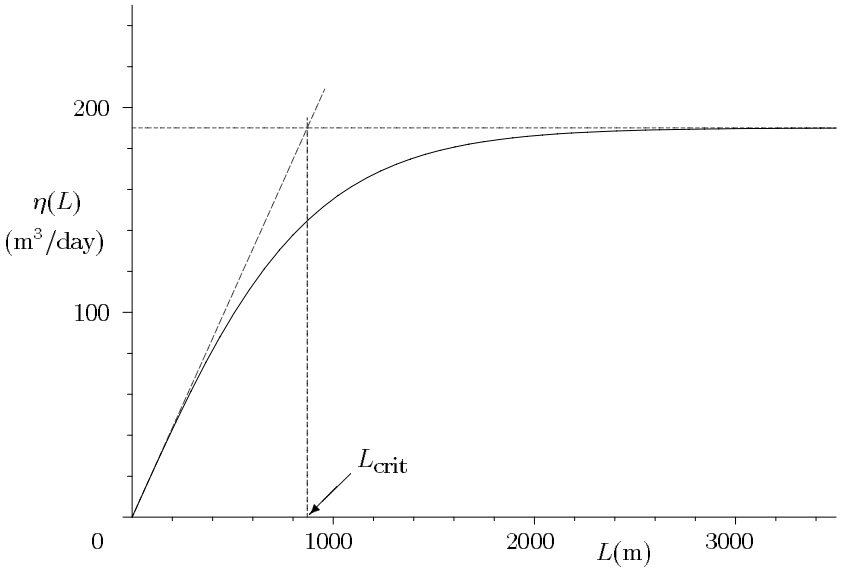

FIGURE 3: The production rate at the pump as a function of the length of the wellbore.

6 Including the temperature. For the purposes of this discussion, we assume that the wellbore has a steady state temperature distribution that is a function of r and z alone. As well, to simplify the expressions, we will take the far field temperature to be zero. We also assume that thermal conduction in the z direction is negligible.

The primary sources of heat are the EMIT regions and the casings around them and it is assumed that the heat production is uniform. Since the reservoir and casings are porous, heat is convected radially in them. In the wellbore, oil flows along the axis and therefore heat is axially convected.

We begin with a justification of ignoring thermal conduction along the wellbore axis. Consider the rate of energy transfer due to convection with that due to conduction. Convection is the dominant process if

$$\rho C_f \bar{v} \delta T \gg \lambda \frac{\delta T}{L}$$

where ρC_f is the specific heat, λ is the thermal conductivity, $\bar{v}$ is the speed of convecting fluid and δT is the change in temperature over the length L. This gives the condition that $\lambda \ll \rho C_f \bar{v} L \sim 5.6 \times 10^7$ W/m/s,

using the data from Table 1 and experimentally observed average speed of $\bar{v} \simeq 0.2$ m/s. Since typical fluids in the wellbore have thermal conductivities of $\lambda \simeq 10$ [**2**], the transport of heat via conduction along the wellbore axis can be safely ignored.

For any of the regions, the heat flux is given by an expression of the form [**2**]

$$\vec{\Phi} = \lambda \nabla u - \rho C_f \vec{v} u$$

where $u = u(r, z)$ is the temperature of a fluid moving with velocity $\vec{v}$. As before, λ and ρC_f are the thermal conductivity and heat capacity of the fluid. In the reservoir and the casing, the fluids are assumed to be flowing at a constant rate of v_o at the drainage radius R_d towards the centre of the wellbore. As such $\vec{v} = -(v_o R_d/r)\hat{\mathbf{r}}$ in these regions. Inside the actual EMIT there is no fluid so that $\vec{v} = \vec{0}$ and in the wellbore we take $\vec{v} = \bar{v}(z)\hat{\mathbf{k}}$ the average radial velocity used in Section 4.

To find the steady state heat equation in each of the regions one has $\nabla \cdot \vec{\Phi} + Q = 0$ where Q is a heat source term (if any) and assuming a steady state. The resulting equations are summarized below:

$$\text{Reservoir:} \quad \frac{1}{r}\frac{\partial}{\partial r}\Big(r\lambda_r \frac{\partial u}{\partial r} + \beta u\Big) = 0 \tag{9}$$

$$\text{Casing:} \quad \frac{1}{r}\frac{\partial}{\partial r}\Big(r\lambda_c \frac{\partial u}{\partial r} + \beta u\Big) + Q_c = 0 \tag{10}$$

$$\text{Wellbore:} \quad \frac{1}{r}\frac{\partial}{\partial r}\Big(r\lambda_w \frac{\partial u}{\partial r}\Big) - \rho C_f \frac{\partial}{\partial z}(\bar{v}u) = 0 \tag{11}$$

$$\text{EMIT:} \quad \frac{1}{r}\frac{\partial}{\partial r}\Big(r\lambda_e \frac{\partial u}{\partial r}\Big) + Q_e = 0 \tag{12}$$

where $\beta = \rho C_f R_d v_o$.

We are not interested in resolving the details of the radial temperature distribution in the wellbore. Rather, we only care about the axial variations of the mean temperature. This permits a simplification. First define the mean temperature over the wellbore cross-section at z to be

$$T(z) = \frac{2}{(R_w^2 - R_z^2)} \int_{R_z}^{R_w} u(r, z) r \, dr$$

as we did with η in the derivation of equation (6). Recall that R_z is the inner radius and depends on z. With this definition, the equation for the wellbore (11) can be integrated, resulting in the expression

$$\rho C_f \frac{d}{dz}(\eta T) = 2\pi r \lambda_w \frac{\partial u}{\partial r}\Big|_{R_z}^{R_w}, \tag{13}$$

again using the fact that $\eta = \pi(R_w^2 - R_z^2)$. The thermal flux in the wellbore is given by

$$\vec{\Phi}_w = \lambda_w \frac{\partial u}{\partial r}\hat{\mathbf{r}} - \rho C_f \bar{v} u \hat{\mathbf{k}}.$$

This must be continuous at the interfaces. Hence in the radial direction for the wellbore/casing and wellbore/EMIT interfaces, one has respectively

$$r\lambda_w \frac{\partial u}{\partial r}\Big|_{R_w} = \left(r\lambda_c \frac{\partial u}{\partial r} + \beta u\right)\Big|_{R_w} \quad \text{and} \quad r\lambda_w \frac{\partial u}{\partial r}\Big|_{R_z} = r\lambda_e \frac{\partial u}{\partial r}\Big|_{R_z}.$$

It remains for us to evaluate these fluxes on the right hand side by using the remaining three heat equations.

For the EMIT region we find by solving (12) that

$$r\lambda_e \frac{\partial u}{\partial r}\Big|_{R_z} = -\frac{1}{2} Q_e R_z^2. \tag{14}$$

Furthermore, by solving (9) one finds that the temperature has the general form

$$u(r, z) = k_1 + k_2 r^{-\beta/\lambda_r}$$

in the reservoir where k_1 and k_2 are constants. Because the far field temperature is zero, one must have $\lim_{r\to\infty} u(r, z) = k_1 = 0$. As a result,

$$r\lambda_r \frac{\partial u}{\partial r} + \beta u = \beta k_1 = 0 \tag{15}$$

and the thermal flux in the reservoir and, in particular, the thermal flux through the casing/reservoir interface, is zero. Using this as a boundary condition one can integrate the expression for the casing (10) to find that

$$\left(r\lambda_c \frac{\partial u}{\partial r} + \beta u\right)\Big|_{R_w} = \frac{1}{2} Q_c (R_c^2 - R_w^2). \tag{16}$$

Collecting equations (13)–(16) gives the final expression

$$\rho C_f \frac{d}{dz}[\eta(z)\, T(z)] = \pi[Q_c(z)(R_c^2 - R_w^2) + Q_e(z) R_e^2]; \quad T(0) = 0. \tag{17}$$

The heat sources Q_c and Q_e have been written as functions of z so that the expression remains valid for the whole length of the wellbore. If one is not in an EMIT region, these functions are simply zero. As a result, the RHS of (17) is piecewise constant, and nonzero only where an EMIT is located.

7 The model. In the axial direction the rate of change of $\eta(z) = \pi(R_w^2 - R_z^2)\bar{v}(z)$ is governed by Darcy's Law, and in our approximation it is assumed that the fluid is not heated until it reaches the wellbore. For the axial pressure the Navier-Stokes equations are solved for an annular region by assuming that the fluid is incompressible. When we apply heat to wellbore, it is this fluid in the wellbore that is heated and not the fluid in the surrounding region. We can summarize the problem for $\eta(z)$ as

$$\begin{aligned} &\frac{d^2\eta}{dz^2} - \gamma^2(z)\frac{\mu(T)}{\mu_o}\eta = 0; \\ &\gamma^2(z) = \frac{16k}{R_w^4 \ln(R_d/R_c)}\Big[\frac{\ln\lambda}{(1-\lambda^2)^2 + (1-\lambda^4)\ln\lambda}\Big], \end{aligned} \tag{18}$$

which is simply (7) with a temperature dependent viscosity. Recall that $\lambda = R_z/R_w$ and R_z is given by expression (2). In the case of one EMIT region the temperature is

$$\begin{aligned} T(z) &= \begin{cases} 0, & 0 \le z < z_e - L_e \\ \dfrac{\Omega}{\eta(z)}\dfrac{z - z_e + L_e}{2L_e}, & |z - z_e| \le L_e \\ \dfrac{\Omega}{\eta(z)}, & z_e + L_e < z \le L, \end{cases} \\ \Omega &= \frac{\pi[Q_c(R_c^2 - R_w^2) + Q_e R_e^2](2L_e)}{\rho C_f}, \end{aligned} \tag{19}$$

found by integrating (17). From the values in Table 1 we find that $\Omega \sim 3.10 \times 10^{-2}$ m^{3}K/s. Notice that if $\eta(z)$ were constant then the temperature would increase monotonically as one moved from $z = 0$ to $z = L$. However, since $\eta(z)$ actually increases as one moves toward the pump, the temperature of the fluid must decrease once it passes an EMIT region.

The temperature affects the velocity and the pressure through the viscosity. This viscosity is given empirically in units of thousands of centipoise through

$$\log_{10}\mu(T) = -3.002 + \Big(\frac{453.29}{303.5 + T}\Big)^{3.5644}, \quad \mu_o = \mu(0). \tag{20}$$

Hence, one can see that an increase of 100°C can result in a decrease in viscosity of about three orders of magnitude. One final point is that

the far field temperature should correspond to the ambient viscosity μ_0. Since $\mu_0 = 15000$ cP we associate the far field temperature of zero with the ambient temperature of $T_a = 30°$C. This last expression for the viscosity and the boundary conditions (8), repeated here for clarity, closes the system

$$\eta(0) = 0, \quad \frac{d\eta}{dz}\Big|_L = \frac{2\pi k(P_R - P_P)}{\mu_o \ln(R_d/R_c)}.$$

Once we have simultaneously solved for $\eta(z)$ and $T(z)$, the pressure as a function of z is determined by expression (3) with the result that

$$P(z) = P_R - \frac{\mu_o}{2\pi k} \ln\Big(\frac{R_d}{R_c}\Big) \frac{d\eta}{dz}. \tag{21}$$

From this relationship one sees that an increase in the flux rate corresponds to a drop in pressure. Therefore, the model should predict a significant pressure drop across an EMIT region where the fluid accelerates due to the decrease in viscosity. Other functions of interest are the average velocity, $\bar{v}(z) = \eta(z)/\big(\pi(R_w^2 - R_z^2)\big)$, and the production rate at the pump, $\eta(L)$.

8 Numerical results. To determine how well the model compares with the results of the commercial code, we first consider the case without an EMIT region and the case with an unpowered EMIT thereby decoupling the temperature effects.

Figure 4 illustrates the pressure profiles in the two cases. In the case with no EMIT the commercial code yields $\eta_{\rm cc}(L) = 153.09$ m^3/day while the simplified model has $\eta_{\rm sm}(L) = 156.03$ m^3/day a difference of 1.9%. With an unpowered EMIT, $\eta_{\rm cc}(L) = 68.89$ m^3/day and $\eta_{\rm sm}(L) = 71.97$ m^3/day a difference of 4.3%. Clearly, good agreement between the two models is demonstrated.

As we have stated back in the introduction, the agreement between the qualitative results of the simplified model and those predicted by the commercial code are quite remarkable. This is especially true in light of their respective computational costs. Figures 5 and 6 illustrate the results for the data described in Table 1.

Only the pressure, temperature and final production rate are easily available from the CFD code. Because of this, only the pressure and temperature curves in Figure 5 have a dashed line. To solve the nonlinear ODE described in Section 7 two different methods were employed,

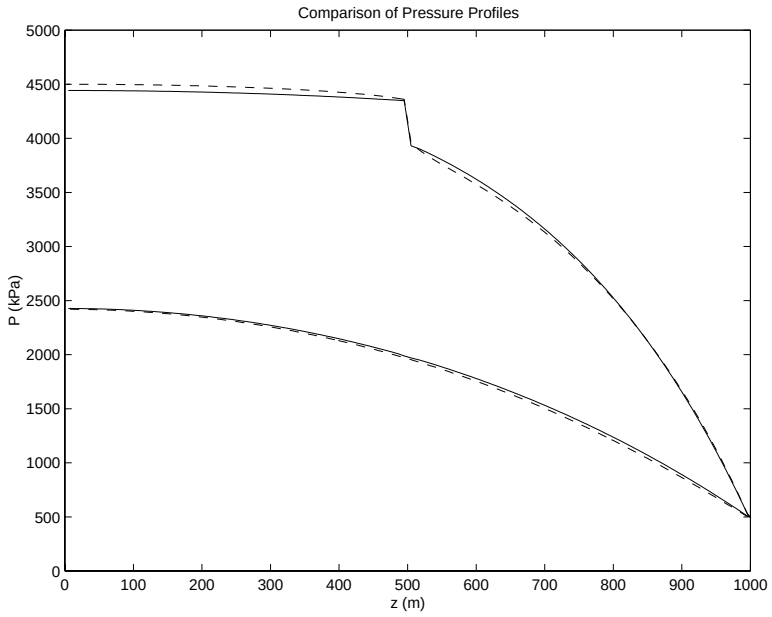

FIGURE 4: Comparison of the pressure profiles with the commercial code. Two cases are shown: (1) with no EMIT and (2) with an unpowered EMIT. The commercial code is indicated with a dashed line whereas our solution has a solid line. The upper curves correspond to the second case. There is good agreement between the two models.

a shooting method and a method of successive over-relaxation (SOR). Whenever they are discernible, the solution from the shooting method is a solid line while the SOR solution is a dashed line. We begin our discussion with the pressure curve.

Because of the boundary condition $P(L) = P_P$, all of the pressure curves intersect at $z = L$. At $z = 0$ the CFD code predicts $P_{\rm cc}(0) = 4.07 \times 10^3$ kPa while the simplified model predicts $P_{\rm sm}(0) = 3.44 \times 10^3$ kPa. Despite the fact that our model tends to underestimate the results from the commercial code, the amount of pressure drop across the EMIT region is predicted correctly. The last curve in this plot is solely for comparison purposes. It is the pressure curve for the example described in Section 5 (no EMIT region).

Comparing the temperature curves, there is a distinct difference in the shape of the two curves. The peak temperature in the EMIT region is faithfully reproduced, but the rate at which the fluids lose heat is larger in the CFD model. Consequently, the surface temperature of

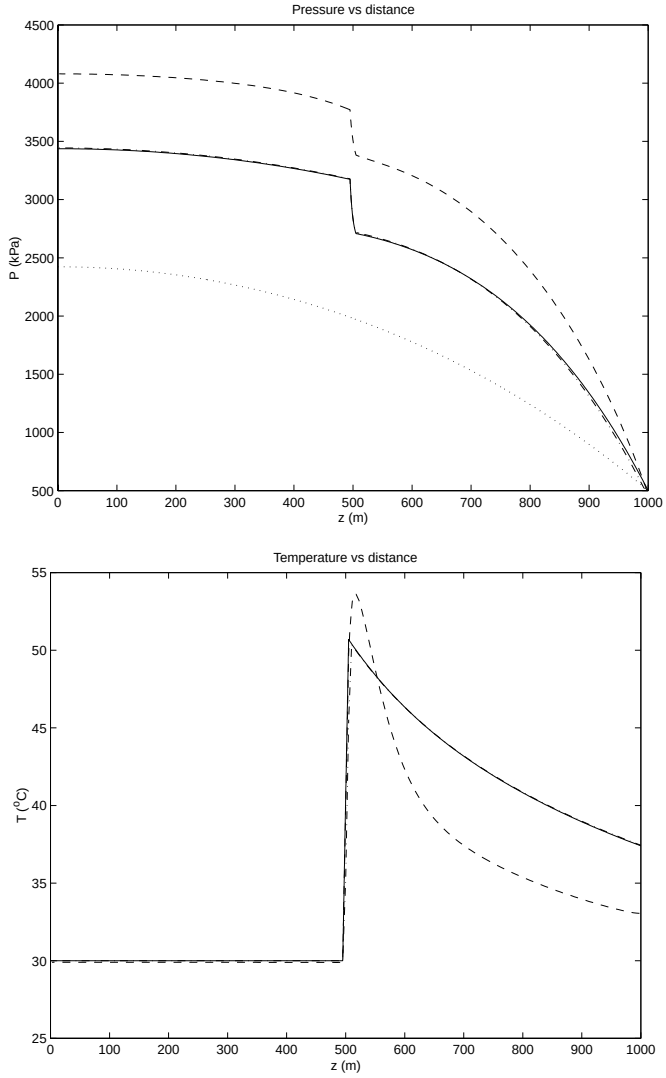

FIGURE 5: The pressure and temperature as a function of distance along the wellbore. For these, the CFD code was available, and are the dashed lines in the respective plots. More than one method was used to solve the simplified model. Where they are distinguishable, the shooting method solution is a solid line where the SOR method is indicated with a dot-dashed line.

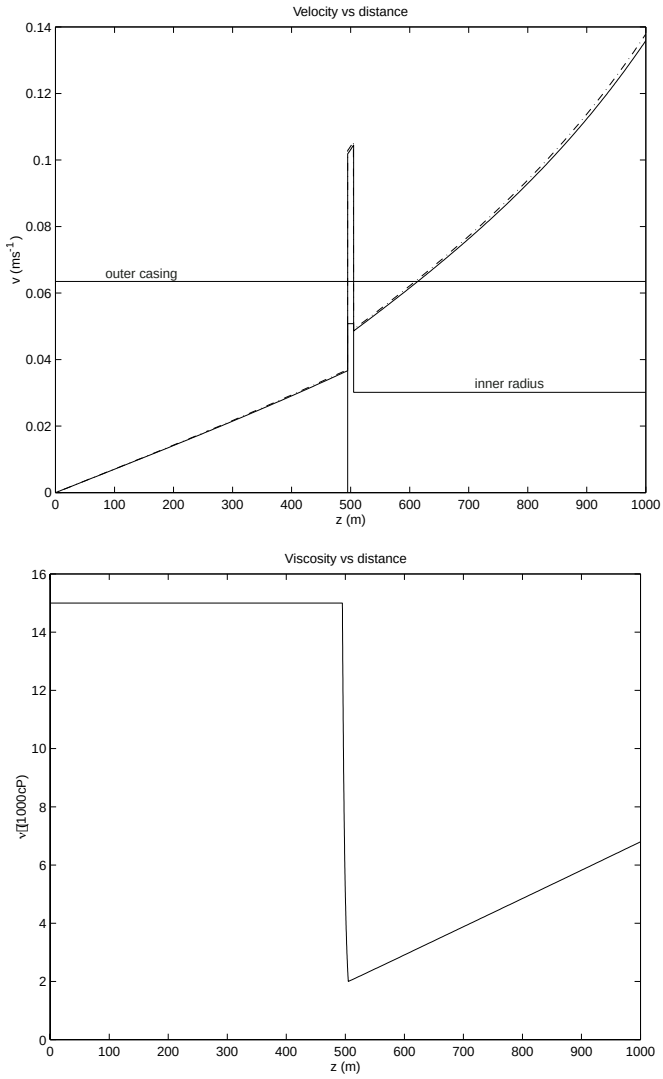

FIGURE 6: The velocity and viscosity as a function of distance along the wellbore. Again, where they are distinguishable, the shooting method solution is a solid line where the SOR method is indicated with a dot-dashed line. A longitudinal section of the wellbore is indicated in the plot of the velocity.

simplified model, $T_{\rm sm}(L) = 37.4^o$C, is larger than that of the CFD model, $T_{\rm cc}(L) = 33.1^o$C. Curves for the viscosity and the velocity could not be compared with the commercial model as these quantities were not directly accessible.

The discrepancies between the commercial model and the simplified model stem from expression (1) and our assumption that the fluid is instantaneously heated when it reaches the wellbore. In actual fact the temperature in the wellbore will increase the flow in the radial direction in a neighbourhood of EMIT. The R_d/R_c ratio in equation (3) defines the radial boundaries of the unheated fluid. Consequently, a crude way to include a thermal boundary is to allow the R_d/R_c in equation (3) to depend on the temperature. Solving the heat equation in the annular region $R_c \leq r \leq R_d$ at a fixed z suggests the replacement:

$$\ln\Big(\frac{R_d}{R_c}\Big) \longrightarrow \ln\Big(\frac{R_d}{r_\epsilon}\Big) = \min\Big\{\frac{T(r_\epsilon)}{T(z)}, 1\Big\} \ln\Big(\frac{R_d}{R_c}\Big)$$

where one fixes $T(r_\epsilon)$ to be some small positive value. Modifying the differential equation (18) and the boundary condition (8) in this manner produces temperature and pressure profiles closer to those of the CFD solution indicating that a careful derivation of the Darcy's Law expression (1) would yield a more robust model.

For the production rate refer to Figure 7. Our model and the commercial package predict similar rates at the pump, specifically, $\eta_{\rm sm}(L) = 115.2$ m^3/day and $\eta_{\rm cc}(L) = 106.5$ m^3/day respectively. Only the flux rate at the pump was available from the CFD code. the dashed curve in this plot is the production rate with no EMIT.

We now turn our attention away from validating the model and investigate the behaviour of the model over various ranges of the parameters.

Figure 8 illustrates the production rate at the pump, $\eta(L)$, as a function of the applied power and the position of the EMIT. The contour on the surface is located at the height corresponding to production rate of $\eta_{\rm sm}(L) = 156.03$ m^3/day, the rate with no EMIT in the wellbore. Since the presence of the EMIT blocks the wellbore, it must be heated to a certain power level to compensate for this effect. With the current geometry this *break-even* point is at about 2000 kW/m^3 and it is attained when the EMIT is placed at the very back of the wellbore. What is also apparent from the surface is that increasing the power level by a small amount to about 2400 kW/m^3, allows one to obtain this break-even point at nearly the midpoint of the wellbore. One final point is that $\eta(L)$ is a stronger function of the power applied to the EMIT than the

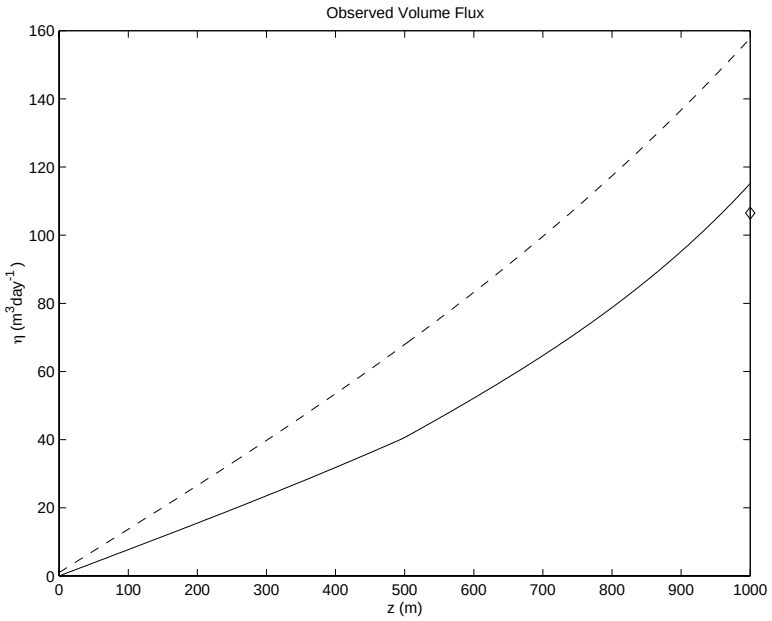

FIGURE 7: The production rate $\eta_{\rm sm}(z)$ as a function of distance along the wellbore for the simplified model. Only the production at the pump $\eta_{\rm cc}(L)$ was available from the CFD code and is indicated with the diamond. The dashed curve is the production rate for the case of no EMIT described in Section 5.

position in the wellbore. One cannot increase the applied power without bound since there is a maximum temperature beyond which the fluids begin to vaporize and the model breaks down [**5**].

The last simulation deals with the situation where a number of EMIT regions are placed in the wellbore and the placement of the EMIT regions is determined so that the viscosity never exceeds some prescribed value. In the case considered, one of the EMITs was fixed at $z = 100$ m and powered with $Q_c = 795.8$, $Q_e = Q_c/10$ and the additional EMITs were given the same power level and placed in the wellbore as they were required. Figure 9 tracks the position of the EMIT regions as the maxiumum allowable viscosity was varied. For example, if $\mu_{\max} = 2000$ cP then four EMIT regions are required and they should be centered at $z = 100$, 315, 598 and 845 m. The EMIT at $z = 100$ was fixed. In this case the production rate was 156.8 m^3/day. While some nonlinear behaviour is apparent, spacing the EMIT regions at equally spaced intervals closely approximates the optimal placing.

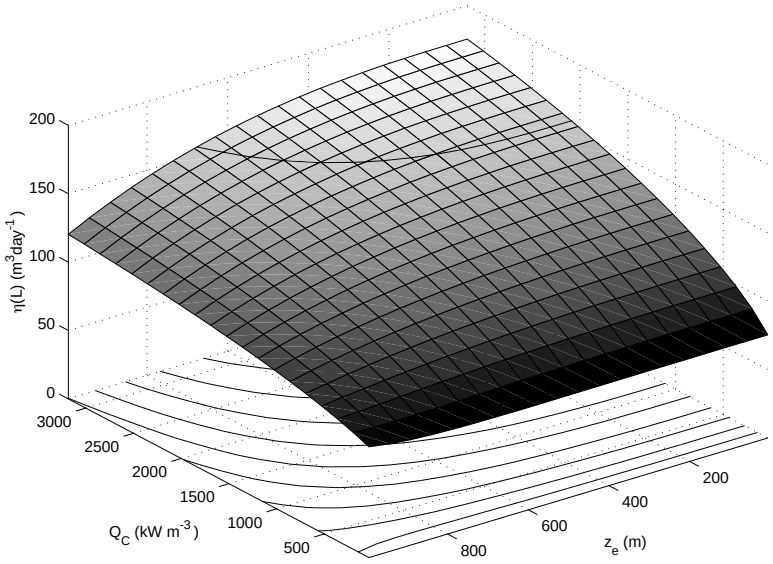

FIGURE 8: The production rate at the pump $\eta_{\mathrm{sm}}(L)$ as a function of the location of the centre of the EMIT, z_e, and the applied power. Rather than using the total power, we simply report the value of Q_c, the power in the casing. We have taken $Q_e = Q_c/10$. The contour on the surface is located at $\eta(L) = 156.03$ m^3/day corresponding to the flux if there was no EMIT.

9 Conclusions. We have presented a mathematical model for the flow of fluids in a horizontal well in which the well has one or more regions that are electrically heated from an external source. By making some basic assumptions and averaging the flow over the cross-section of the wellbore, we developed a nonlinear second order *ordinary* differential equation for the volume flux $\eta(z)$ as a function of distance along the wellbore. From the volume flux, both the average radial temperature and the pressure can be extracted. Comparing the predictions with those from an expensive computational fluid dynamics (CFD) program we find that the simplified model captures many of the features observed in the solution to the full PDE system. A simple modification of the model to account for a thermal boundary layer reduces the differences between the two models.

Despite these criticisms, the predicted production rates correspond with those of a full CFD solver seem to validate the model. The large

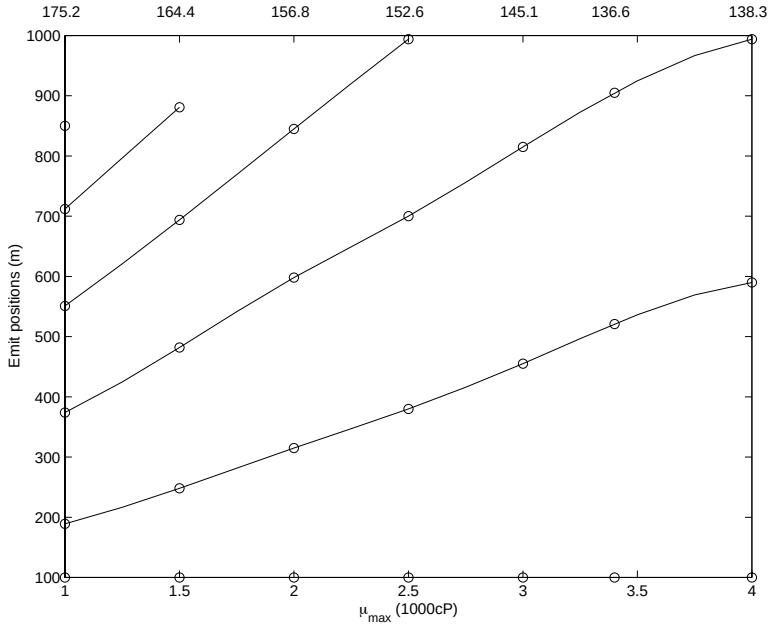

FIGURE 9: Position of the EMIT regions as a function of the maximum allowable viscosity, $\mu_{\max}$. Each value of $\mu_{\max}$ considered has a corresponding production rate $\eta(L)$ These values are illustrated above their respective values of $\mu_{\max}$.

reduction in computational cost when using the simplified model allows one to quickly run a series of numerical experiments to see the effects of changing various parameters. Two such experiments are considered. First, the production rate at the pump as a function of both the applied power and the position of the EMIT and second, the optimal positioning of the EMIT regions as a function of the maximum allowable viscosity.

Acknowledgement The authors would like to thank PIMS and the Applied Math Institute of Alberta.

REFERENCES

1. L. D. Landau and E. M. Lifshitz, *Fluid Mechanics*, Addison-Wesley Series in Advanced Physics, Pergamon Press Ltd., Reading, Massachusetts, 1959, 56–57.
2. J. H. Lienhard, *A Heat Transfer Textbook*, Prentice-Hall, Inc., New Jersey, 1987.

3. M. K. Hubbert, *Darcy's Law and the Field Equations of the Flow of Underground Fluids.* Petroleum Transactions–AIME **207** (1956), 222–239.
4. T. Myint-U, *Partial Differential Equations in Mathematical Physics*, American Elsevier Publishing Company, Inc., New York, 1973.
5. P. K. W. Vinsome, B. C. W. McGee, F. E. Vermeulen and F. S. Chute, *Electrical Heating*, J. Can. Pet. Technol. **33** (1994), 29–35.

Department of Mathematics, The Pennsylvania State University,
1 Campus Drive, Mont Alto, PA 17237
E-mail address: csb15@psu.edu

McMillan-McGee Corp., 4450-46th Avenue SE, Calgary, Alberta,
Canada T2B 3N7
E-mail address: mcgee@mcmillan-mcgee.com

Applied Mathematics and Statistics Group, Eastman Kodak Company,
Rochester, NY 14650-2205
E-mail address: ross@kodak.com